Understanding reactions with O_2 for ^{90}Sr measurements by ICP-MS with collision-reaction cell

Georges Favre [a,*], René Brennetot [a], Frédéric Chartier [a], Pierre Vitorge [b]

[a] *Laboratoire d'Analyses Nucléaires Isotopiques et Elémentaires, Bât. 391, Commissariat à l'Energie Atomique, Centre d'Etudes de Saclay, 91191 Gif-sur-Yvette Cedex, France*
[b] *Laboratoire de la Spéciation des Radionucléides et des Molécules, Bât. 391, Commissariat à l'Energie Atomique, Centre d'Etudes de Saclay, 91191 Gif-sur-Yvette Cedex, France*

Abstract

Inductively coupled plasma mass spectrometry (ICP-MS) is used for the analysis of strontium whose radionuclide ^{90}Sr, present in spent nuclear fuel, is a high beta radiation emitter. Such a measurement is however interfered by the presence of ^{90}Zr, a fission product and a component of the sheath in nuclear industry, at the same mass to charge ratio *m/z*. Collision-reaction cells allow to suppress this isobaric interference by using O_2 as a reaction gas. This process has been extensively experimentally studied by others. However, the modeling of gas–ions interactions is also of prime interest in understanding and forecasting the behavior of species in the cell. Quantum calculations using density functional theory (DFT) were then performed on the species involved in the reactions with O_2 leading to the suppression of the ^{90}Zr/^{90}Sr interference. Indeed, the 1 ms mean residence time of ions in the cell leads to a thermalized ion beam, what allows using this modeling method. A systematic study of the equilibrium geometries and of the electronic structures was carried out. Differences in the nature of chemical bonding in zirconium and strontium oxides were then highlighted for explaining the opposite behavior of Sr and Zr ions towards oxygen. In addition similar OM^+–O connectivity within MO_2^+ was observed for both ZrO_2^+ and SrO_2^+ dioxides. Computed O-atom affinities, OA, and reaction enthalpies of the oxidation processes, ΔH_r, were compared with available experimental data, while a first determination of the SrO_2^+ formation enthalpy, $\Delta H_f(SrO_2^+)$, at 846 kJ mol^{-1} was possible from these DFT calculations, when no value was found in the literature.
© 2007 Elsevier B.V. All rights reserved.

Keywords: ICP-MS; DFT calculations; Zirconium; Strontium; Interference; O_2

1. Introduction

Precise inventory of fission products present in spent nuclear fuel is crucial for the nuclear industry, typically for qualifying neutronic codes currently used for the management of nuclear irradiated fuel and related safety analysis. Strontium-90 ($T_{1/2} = 28.8$ years) is an important fission product generated in nuclear industry, which emits highly energetic beta radiations. Because of its impact in both environmental and health areas its accurate and precise quantification is of prime interest in nuclear, natural or medical samples.

In most of cases radiometric determination of ^{90}Sr presents a challenge due to interferences from other beta-emitters, particularly its daughter isotope, ^{90}Y. Accurate beta counting therefore requires isolation of ^{90}Sr from other beta-emitting isotopes, followed by ingrowth of ^{90}Y ($T_{1/2} = 64$ h) until secular equilibrium is reached ($\sim$15 days), and sufficiently long counting times to obtain acceptable precision [1]. This results in time consuming measurement processes. A faster quantification technique, such as mass spectrometry where same day preparation and analysis of samples are achievable, becomes advantageous when a large number of samples require analysis, even if it does not reach detection limits of radiometric counting. Isotope dilution coupled with mass spectrometry is a method that can provide accurate measurement of radioactive ^{90}Sr [2]. However, the use of mass spectrometry techniques for measuring ^{90}Sr suffers from a different set of analytical challenges from those associated with beta counting: isobaric interferences due to the

* Corresponding author. Tel.: +33 169081848; fax: +33 169085411.
E-mail addresses: georges.favre@cea.fr (G. Favre), rene.brennetot@cea.fr (R. Brennetot), frederic.chartier@cea.fr (F. Chartier), pierre.vitorge@cea.fr (P. Vitorge).

presence of ^{90}Y and ^{90}Zr in all types of samples to analyze and sometimes high concentrations of natural strontium (stable ^{88}Sr) which require to consider the participation of the peak tail of ^{88}Sr in the ^{90}Sr signal. While the presence of yttrium-90 in the fuel sample is negligible (only 0.02% of the total intensity) [2], ^{90}Zr, component of the sheath in the nuclear industry and also stable daughter isotope of ^{90}Y, is present in great proportions (20% of the total intensity at m/z 90). Different possibilities can be envisaged to remove completely the stable isobar ^{90}Zr to below-background intensity at m/z 90. Chromatographic separation of strontium from interfering elements before analysis by Thermal Ionization Mass Spectrometry (TIMS) [2] for example is a classical way used in most cases. But it presents also drawbacks proper to the nuclear field with the increase of (1) the risk of natural contamination, (2) handling time on radioactive solutions and (3) radioactive wastes. Several analytical approaches exist to avoid such supplementary step and lower irradiation of operators. The double focusing Sector Field Inductively Coupled Plasma Mass Spectrometry (ICP-SFMS) is an effective tool which may provide a sufficiently high resolution for separating ions differing in mass by a fraction of a mass unit, as in the case of the ^{90}Zr/^{90}Sr isobaric interference (mass of ^{90}Zr = 89.9047 uma and ^{90}Sr = 89.9077 uma) [3,4]. But the required mass resolution ($m/\Delta m = 30{,}000$), beyond actual possibilities, and the purchase price of such apparatus constitute a major obstacle which explains the development of others solutions. Cold plasma has been examined for taking advantage of the differences in ionization potential (IP(Zr) = 639.2 kJ mol^{-1} and IP(Sr) = 561.8 kJ mol^{-1}) [3], but such plasma conditions enhance the formation of matrix-derived polyatomic ions and sensitivity becomes particularly dependent on the matrix of the sample [5]. As a result, the use of ICP-MS with collision-reaction cells is increasingly widespread to avoid the chromatographic step and lower irradiation of operators. Interferences can be thus reduced or even eliminated by addition of a reaction gas in the cell [6].

When available, thermodynamics data are used to calculate energies of reactions, which allow to select the reaction gas. In fact, the true discriminator of a thermodynamically allowed gas phase reaction is the "Gibbs energy of reaction", ΔG_r, which takes into account an entropy term ($\Delta G_r = \Delta H_r - T\Delta S_r$). But in most cases the entropy of bimolecular reactions can be neglected in the gas phase [6]. We shall use this approximation. Under those circumstances the enthalpy of reaction, ΔH_r, is the criterion used for predicting feasibility of the reactions. Chemical resolution will be achieved, when the reacting gas is chosen such that it has an exothermic channel with either the analyte ion or the isobaric interference ion [6,7].

Eiden et al. first reported the use of O_2 in reaction cell for the resolution of the ^{90}Zr/^{90}Sr interference. Many experimental studies on O-atom transfer reactions [2,8–10] have been then published to show the efficiency of gas phase reaction of Zr with O_2, leaving m/z 90 free of interference. However, the use of collision-reaction cells is not at present completely optimized, neither is the nature of chemical bonding in zirconium and strontium oxides completely understood. Quantum chemistry

calculations are currently used for studying ion–molecule reactions in the gas phase since the systems to model are relatively small and there is no solvent to consider.

Here, we have used a density functional theory (DFT) method for determining the electronic configuration and the geometry, at their ground state, of the oxides formed in the cell. The comparison of our computed results to available experimental data led us to augment the basis set initially used in the calculations for obtaining a better agreement between the values. The formation enthalpy of strontium dioxide has been evaluated and differences in the electronic structure of the bonding in strontium and zirconium oxides have been advanced to explain the opposite behavior of the two elements towards oxygen.

2. Methods, computational details and preliminary calculations

2.1. Material and reagents

The experiments were carried out with a quadrupole ICP-MS X7 (THERMO ELECTRON, Winsford, UK) equipped with collision cell technology (CCT). The Ar plasma – in which the sample is nebulized – is provided by the application of a 1400 W radio frequency potential (RF).

This ICP-MS has been modified in order to work with radioactive materials. A glove box (JACOMEX, Dagneux, France) has been installed for this purpose. The nebulizer, the peristaltic pump, the plasma ion source, and the interface are located in the glove box. An autosampler CETAX ASX 260 also situated in the glove box and controlled by the PlasmaLab software (Thermo Electron) minimizes human irradiation. Airtightness is ensured by a modified interface, and the pumping system was also adapted. A new pump was added (EDWARDS 65 m^3 h^{-1}) from the standard configuration to ensure a better vacuum in the expansion, and to compensate the head losses due to the addition of filters.

Two independent cooling systems were used: the first one for the spray chamber (maintained at 3 °C by Peltier effect), and the second one for the interface and the RF coil.

A multi element tuning solution (SPEX) was used every day for the instrument optimization, and for short term stability tests. All the experiments have been performed on the most abundant natural zirconium and strontium isotopes, ^{90}Zr and ^{88}Sr, with 1 ng mL^{-1} zirconium and strontium solutions. These solutions have been obtained from 1 μg mL^{-1} stock solutions prepared from 1000 μg mL^{-1} natural strontium and zirconium solutions (SPEX) diluted in 0.2 mol L^{-1} nitric acid. The 0.2 mol L^{-1} nitric acid solution was prepared by diluting a 65% Normatom PRO-LABO solution with milliQ (Millipore) water (18.2 MΩ cm conductivity).

High purity oxygen (6.0–99.9999% purity) was obtained from MESSER France, and used as reaction gas for the experiments in the pressurized mode. Intensities on strontium and zirconium species were followed for different molecular oxygen flow rates. The instrumental parameters were adjusted for having the maximum signal intensity on the most abundant ion

(always Sr^+ for strontium and ZrO^+ when O_2 is introduced in the cell).

2.2. Method

Quantum calculations were performed with the Gaussian03 suite of programs [11] at Hartree–Fock and density functional theory (B3LYP [12]) levels. Two different basis sets and associated pseudo-potential (SDD [13] and LanL2DZ [14]) as available in Gaussian03 were tested on monoatomic ions. In a first step, the energies of geometrically optimized species were compared to determine the calculation level and the ground state spin multiplicities. Natural Bond Orbital (NBO) calculations were also performed as implemented in Gaussian03.

The spin contamination, SC, was used for checking the consistency of the calculations.

Thermal corrections were used as implemented in Gaussian03, here for obtaining standard state enthalpy, H, and Gibbs energy, G, at 298.15 K, 1 atm, even if the pressure is definitely lower in the cell. O-atom affinities and reaction enthalpies have been calculated from these values. Since some of them poorly predicted experimental data the LanL2DZ basis set was made flexible and augmented. Contraction coefficients of added functions were all taken equal to 1. The experimentally known bond dissociation energy of O_2, $D(O–O)$, and ionization potentials, IP, of Zr and Sr [15], were used as the optimization criteria of the exponential coefficients. Addition of a polarization function d (optimized exponential coefficient: 1) on the flexible Lanl2DZ basis set for O atom already improved $D(O–O)$. The diffuse function p (optimized exponential coefficient: 0.01) refined $D(O–O)$ to 497.5 kJ mol^{-1} for a 498 kJ mol^{-1} expected value, whereas it is underestimated by 104 kJ mol^{-1} with the Lanl2DZ basis set. Concerning augmented basis set for Zr and Sr atoms the addition of f and d diffuse functions (optimized coefficients 0.6 and 0.3, respectively), leads to IP values in better agreement with the experimental data (Table 1). The ionization potentials are indeed overestimated for Zr and Sr with the Lanl2DZ basis set by 22.0 and 20.7 kJ mol^{-1}, respectively. The basis set thus obtained is referenced in this paper as Lanl2DZ++* with the usual notation (++ for diffuse functions on all atoms and * for polarization functions).

However, the formation enthalpy of ZrO^+, $\Delta H_f(ZrO^+)$, was still overestimated by using our basis set. A basis set superposition error (BSSE) calculation was carried out with Lanl2DZ++* on reaction (1) to evaluate the counterpoise correction. Besides, correct DFT results were obtained for reaction (2). The reaction of interests for us in the cell is obtained by linear combination: (3) = (1) − (2). The counterpoise correction for reaction (3) is

thus also simply evaluated.

$$M^+ + O \rightarrow MO^+ \tag{1}$$

$$2O \rightarrow O_2 \tag{2}$$

$$M^+ + O_2 \rightarrow MO^+ + O \tag{3}$$
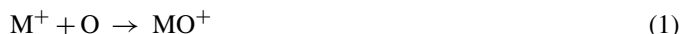
This BSSE appeared to be small (<6 kJ mol^{-1}). We did not take it into account. An *ab initio* method (Quadratic Configuration Interaction with Single and Double Excitations, QCISD) was also used in an attempt to improve the quantum description of ZrO^+.

The molecular graphics package MOLEKEL [16,17] was used for visualizing electronic structure data.

Equilibrium constant K (or equivalently the corresponding Gibbs energy of reaction, ΔG_r) is classically interpreted as the activity of the exchanged reactant at the half point reaction (classically $pK_a = pH_{1/2}$ for H^+ exchange reactions). However, in our case the exchange species can be O_2. Determination of the O_2 partial pressures, P_{O_2}, at the half point of the O_2-condensation reaction (4), where the M^+ and MO_2^+ partial pressures are equal, gives an intuitive approach of the reactivity of oxygen towards Zr^+ and Sr^+.

$$M^+ + O_2 \rightarrow MO_2^+ \tag{4}$$

$[P_{O_2}]_{1/2}$ is easily evaluated since the equilibrium constant K only depends on the oxygen partial pressure:

$$[P_{MO_2^+}]_{1/2} = [P_{M^+}]_{1/2} \rightarrow K = \frac{1}{[P_{O_2}]_{1/2}} \tag{a}$$

with $[P_i]_{1/2}$ the different partial pressures at the half point of reaction (4). K was determined by using the mass action law (b) where ΔG_r was deduced from our DFT calculations, R the ideal gas constant (8.314 J K^{-1} mol^{-1}) and T_{cell} is the temperature in the cell.

$$\Delta G_r + RT_{cell} \ln K = 0 \tag{b}$$

3. Results and discussion

A recently work published by Rondinelli et al. [18] focused on the theoretical approach of reactions between Zr^+ and CO_2 with a view to convert carbon dioxide into a non-dangerous species for the atmosphere. The calculations were carried out with several exchange-correlation functionals, in particular B3LYP used in our work, in connection with 6-311++G** basis set and Lanl2DZ pseudo-potential. Geometrical data on zirconium oxides and energetic values reproducing experimental data are presented by the authors. They found for ZrO^+ a doublet ground state ($^2\Sigma^+$) with a Zr^+–O distance value of 1.734 Å followed by the first excited state of quartet ($^4\Phi$) with a 1.955 Å Zr^+–O bond length. Concerning ZrO_2^+ dioxide an electronic ground state of doublet was reported with the two Zr^+–O bond lengths at 1.818 Å and the O–Zr^+–O valence angle equal to 94.25°. Reported results about the reactions mechanisms between CO_2 and zirconium species are in agreement with the experimental predictions from a qualitative point of view. But heats of reaction values calculated in order to check the theoretical method and level are

Table 1
Comparison of basis sets (energies in kJ mol^{-1}, B3LYP method)

	Experimental[a]	Lanl2DZ	Lanl2DZ++*
$D(O–O)$	498	393.6	497.5
$IP(Zr)$	639.2	661.2	637.7
$IP(Sr)$	561.8	582.5	556.6

[a] Ref. [15].

lower than the experimental determination often by more than $50 \, \text{kJ} \, \text{mol}^{-1}$ when the B3LYP/6-311++G**/LANL2DZ protocol was used because of the underestimation of ZrO$^+$ computed energy.

3.1. Monoatomic ions

Two spin multiplicities ($S = 2$ or $S = 4$) are possible for Zr$^+$ ([Kr] $4d^2 5s^1$), and only one is conceivable ($S = 2$) for Sr$^+$ ([Kr] $5s^1$). For Zr$^+$ all calculation levels give lower energies for the highest spin multiplicity $S = 4$ than for $S = 2$. $S = 4$ is the more stable state as also reported in Rondinelli's paper [18]. This is confirmed by the spin contamination, and it is consistent with the Hund's rules.

B3LYP/LanL2DZ level was used for calculation of others species since Lanl2DZ basis set and associated pseudo-potential are more extended than the SDD ones.

3.2. Oxide ions

Addition of an oxygen atom dramatically modifies the electronic configurations of the ions. ZrO$^+$ and SrO$^+$ conceivable spin multiplicities are deduced from those of Zr$^+$ and Sr$^+$. The following values can be considered for spin multiplicity of ZrO$^+$ depending on how the electrons are distributed on zirconium and oxygen orbitals: 2, 4, 6, 8 and 10. Three spin multiplicity values are possible for SrO$^+$: 2, 4 and 6.

Table 2 gives the energy, E, and the equilibrium internuclear distance, R_e, for each considered spin multiplicity value of zirconium and strontium monoxide ions at their optimized geometry. $S = 8$ and $S = 10$ were rejected since they correspond to high equilibrium internuclear distance, which reflects poor Zr–O binding. Moreover, calculated energies are the highest, what confirms that these two spin states do not correspond to stable ZrO$^+$ molecular ion. This is also the case for the $S = 6$ spin value of SrO$^+$. In all the cases above-mentioned the instability is originated in the unpairing of 2s and 2p oxygen electrons to obtain these spin multiplicities for which no bond is formed between the M$^+$ and O atoms. Among the remaining S values of ZrO$^+$ and SrO$^+$ ions, the lowest energies and the shortest R_e are found for the spin

Fig. 1. Comparison of ZrO$^+$ electronic density for different spin multiplicities (Zr atom is on the top of the scheme and O atom that of bottom).

multiplicity $S = 2$, which consequently corresponds to the most stable state of both oxides.

Distributions of valence electrons for the above remaining S values of each oxide were also examined through NBO calculations. This complementary study allowed to confirm the spin of ZrO$^+$ and SrO$^+$ ground state and to bring a clarification on the bonding in these species. Fig. 1 shows that only the $S = 2$ spin state clearly leads to the formation of a covalent bond in ZrO$^+$. The electronic density is indeed quasi-uniform between the two atoms, while for $S = 6$ a nodal zone can almost be observed. Associated numerical results (Table 3) illustrate that the 5s valence electron of the zirconium is transferred to the oxygen for the spin multiplicity $S = 2$, corresponding to an intramolecular oxidation of zirconium by oxygen. Conversely, Zr$^+$ and O electronic distributions are not altered by forming ZrO$^+$ for $S = 6$, consistent with no charge transfer hence no covalent bonding. The spin multiplicity $S = 4$ corresponds to an intermediate situation, where only half an electron is transferred from zirconium to oxygen. Looking more precisely to the bond orbital analysis gives an explanation about the shape of the electronic densities and the difference in bond lengths. Indeed we observed a very polarized triple bond for the spin value $S = 2$, while the case $S = 4$ presented only a single bond between Zr and O, less polarized toward the O atom. The corresponding σ-bonding orbital is mainly made from a Zr $5s4d_{z^2}$/O $2s2p_z$ hybrid orbital, while the $S = 2$ spin configuration presents quasi-pure Zr $4d_{xz}$/O $2p_x$ and Zr $4d_{yz}$/O $2p_y$ additional π-bonding orbitals, leading to a more

Table 2

Comparison of ZrO$^+$ and SrO$^+$ optimized energy, E, and equilibrium internuclear distance, R_e, for different spin multiplicities at the calculation level B3LYP/LanL2DZ (energies, E, in Hartrees, R_e in Å)

	S	δE	δR_e
ZrO$^+$	2	0.000	0.00
ZrO$^+$	4	0.103	0.16
ZrO$^+$	6	0.200	0.90
ZrO$^+$	8	0.481	2.03
ZrO$^+$	10	0.471	2.06
SrO$^+$	2	0.000	0.00
SrO$^+$	4	0.059	0.98
SrO$^+$	6	0.432	2.85

E_{ref}(ZrO$^+$) = −121.482 Hartree, R_e(Zr–O)$_{ref}$ = 1.74 Å, E_{ref}(SrO$^+$) = −105.360 Hartree, R_e(Sr–O)$_{ref}$ = 2.35 Å.

Table 3

Natural population analysis[a] of ZrO$^+$ and SrO$^+$ (bond length in Å)

Spin multiplicity	$S = 2$	$S = 4$	$S = 6$
ZrO$^+$	Zr $4d^{2.20} 5s^{0.00}$ O $2s^{2.00} 2p^{4.80}$	Zr $4d^{2.20} 5s^{0.30}$ O $2s^{2.00} 2p^{4.50}$	Zr $4d^{2.60} 5s^{0.40}$ O $2s^{2.00} 2p^{4.00}$
Zr$^+$ O		$4d^{2.00} 5s^{1.00}$ $2s^{2.00} 2p^{4.00}$	
Bond length	1.74	1.90	2.64

Spin multiplicity	$S = 2$		$S = 4$
SrO$^+$	Sr $4d^{0.00} 5s^{0.20}$ O $2s^{2.00} 2p^{4.80}$		Sr $4d^{0.00} 5s^{1.00}$ O $2s^{2.00} 2p^{4.00}$
Sr$^+$ O		$4d^{0.00} 5s^{1.00}$ $2s^{2.00} 2p^{4.00}$	
Bond length	2.35		3.33

[a] NBO: B3LYP/LanL2DZ.
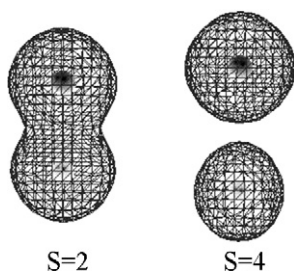
Fig. 2. Comparison of SrO⁺ electronic density for different spin multiplicities (Sr atom is on the top of the scheme and O atom that of bottom).

Fig. 3. Comparison of ΔE_r for the O_2-condensation reaction (4) for Zr and Sr and a $[0-180°]$ O–M–O angle variation (B3LYP/LanL2DZ).

uniform electronic distribution. Only lone pair electrons were found for the case $S = 6$ of ZrO⁺, evidencing no bonding; the high value calculated for the equilibrium internuclear distance ($R_e = 2.64$ Å) brings additional evidence to this fact. Consistently with these observations the Zr–O bonding is stronger for $S = 2$ than for $S = 4$ leading to a lower energy and also a shorter bond length in agreement with the value reported by Rondinelli et al. (respectively, $R_e = 1.74$ Å and $R_e = 1.90$ Å, Table 3). This result is consistent with experimental works [19–22], that determined a spin multiplicity of 2 for the electronic ground state of ZrO⁺. This gives confidence in our DFT calculations.

For SrO⁺ it is obvious thanks to the representation of the electronic densities (Fig. 2) that the spin multiplicity $S = 4$ does not correspond to a binding situation as envisaged above. Indeed, the internuclear distance associated to $S = 4$ ($R_e = 3.33$Å) is larger than for $S = 2$ ($R_e = 2.35$ Å), and the Sr⁺ and O electronic distribution are virtually not altered by the formation of SrO⁺ (Table 3) leading to a nodal zone between strontium and oxygen atoms. The bond orbital analysis confirmed this conclusion since only lone pair electrons, evidencing no bonding, composed the valence electrons. Conversely for the ground state $S = 2$, Sr⁺ gives almost one 5s valence electron to O. Thus, a polarized single bond characterizes this spin configuration of the ground state of SrO⁺. The shape of the electronic density is moreover similar to that of ZrO⁺ $S = 4$. Strontium monoxide presents only a weakly covalent bond as compared to ZrO⁺ ($S = 2$, Fig. 1). The comparison of Sr–O and Zr–O respective bond lengths ($R_e = 2.35$ Å versus 1.74 Å) is also consistent with this difference in bonding, which explains the stronger binding character of oxygen with zirconium than with strontium.

Adding a supplementary oxygen atom again modifies the ion electronic configurations. ZrO₂⁺ and SrO₂⁺ possible spin multiplicities are deduced from those of ZrO⁺ and SrO⁺. Spin values $S = 2$ and 4 have been considered for each ionic species. The energy of ZrO₂⁺ is lower, therefore corresponds to a more stable state, for $S = 2$ than for $S = 4$ ($\delta E = 300$ kJ mol⁻¹). This is the same electronic configuration as obtained by Sievers and Armentrout [21], based on theoretical calculations [23] for the isovalent YO₂ neutral molecule, for which they found a $^2\Sigma^+$ ground state. SrO₂⁺ ground-state corresponds to the value $S = 4$ ($\delta E = 50$ kJ mol⁻¹). Spin contamination associated to the calculation of $S = 2$ is very high (SC > 13%) compared to that obtained for $S = 4$ (SC < 0.1%) consistent with SrO₂⁺ stable state determination. The study of the equilibrium geometry of ZrO₂⁺ and
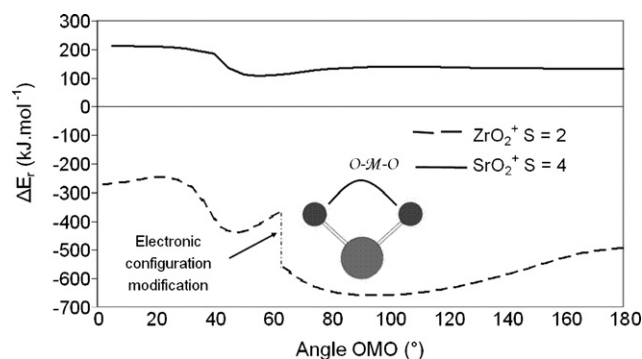
SrO₂⁺ was then carried out (Fig. 3) by modifying the value of the O–M–O angle between 0 and 180°. A symmetric structure was found for both dioxides (d(Zr–O) = 1.82 Å and O–Zr–O = 94.8°, d(Sr–O) = 2.47 Å and O–Sr–O = 55°) and the results on ZrO₂⁺ dioxide are in excellent agreement with those published by Rondinelli. This OM⁺–O connectivity within MO₂⁺ (M = Zr or Sr), predicted by our DFT calculations, is consistent with the collision induced dissociation studies [9] which indicated the detachment of O-atom and not the loss of O₂ molecules as on others dioxides (ReO₂⁺, PtO₂⁺).

3.3. Comparison with experimental energies

Oxygen atom transfer reactions (3) and (4) are the main reactions occurring in the cell when O₂ is used as the reaction gas. They have been largely experimentally studied for the resolution of the interference between ⁹⁰Zr and ⁹⁰Sr [2,8–10]. Eiden et al. first gave results on the different reactivities of molecular oxygen towards zirconium and strontium. They showed that Zr⁺ completely reacts with O₂, and consequently has an exothermic behavior ($\Delta H_r < 0$). This also shifts the ⁹⁰Zr interfering ion to the mass 106 or 122, evidencing the formation of ZrO⁺ and ZrO₂⁺. Conversely Sr⁺ did not react ($\Delta H_r > 0$) unless additional energy was provided to the process (by the radio frequency potential RF for example) [24].

The energies calculated at the B3LYP/Lanl2DZ level are used hereafter for obtaining different thermodynamic values, such as the O-atom affinities, OA, whose values allow anticipating the different behaviors of the elements towards O₂. The computed results were then compared to previous experimental determinations [15,20]. It appeared immediately that some of them poorly predicted experimental data (Table 4) as previously mentioned by Rondinelli et al. [18] Indeed, the oxygen affinities of Zr⁺ and Sr⁺ are underestimated by, respectively, 142 and 126 kJ mol⁻¹ when calculated with the Lanl2DZ basis set. This problem is actually partially originated in the underestimation of $\Delta H_f(O)$ by up to 100 kJ mol⁻¹. The Lanl2DZ basis set used for calculation of O and O₂ presents indeed only s and p contracted functions which take no account of the important polarization effect due to the approach of electron lone pairs of the two oxygen atoms. Thus, this difference propagates

Table 4
Oxygen affinities, OA, for Zr^+, Sr^+ and their oxides (in kJ mol^{-1})

		Zr^+	Sr^+	ZrO^+	SrO^+
OA	Experimental	748 ± 10.5[a]	299[b]	390 ± 10.5[c]	na[d]
	Lanl2DZ	606	173	459	118
	Lanl2DZ++*	685	283	462	83

[a] Ref. [20].
[b] Ref. [28].
[c] Deduced from Refs. [15,20].
[d] No value is published.

into the others thermodynamic quantities, such as the enthalpies of the reactions involving ZrO^+ and SrO^+. We focused on the enthalpy of reaction (1) to evaluate the validity of zirconium and strontium monoxides calculation, since there is no energy problem with the other species involved in the reactions. The use of our augmented basis set Lanl2DZ++* gave computed O–O bond dissociation energy, $D(O–O)$, and enthalpies in much better agreement with experimental data ($\delta E_{max} < 16$ kJ mol^{-1}), excepted again for the ZrO^+ formation enthalpy, $\Delta H_f(ZrO^+)$. Indeed the difference between reaction (1) experimental and computed values is still above 60 kJ mol^{-1}, and using others basis sets available in Gaussian03 (DZVP [25], WTBS [26], CRENBL ECP [27]) did not specially improve the calculated energies. The experimental ZrO^+ energy values are definitely badly reproduced with the DFT method even with an optimized basis set, which suits all the other species here studied. By now no completely acceptable reason was found to explain this discrepancy even if Rondinelli et al. reported that the energetic gap between ground and excited states of zirconium ion computed at DF level ($Zr^{+4}F–^2D$ gap) is underestimated with the B3LYP method. Using the *ab initio* quadratic configuration interaction with single and double excitations (QCISD) method did not specially improve the value obtained for $\Delta H_f(ZrO^+)$ ($\delta\Delta H \approx$ a few kJ mol^{-1}), O_2 being furthermore badly calculated. The enthalpy calculated for reaction (3) was indeed equal to -211 kJ mol^{-1} for an experimental determination at -249 kJ mol^{-1}, but the corresponding $D(O–O)$ value that best fit the experimental data was underestimated by 100 kJ mol^{-1}.

The oxygen affinity of zirconium, OA(Zr^+), was previously calculated by Sievers and Armentrout [20,21] from analysis of the reaction cross sections and by Koyanagi et al. with inductively coupled plasma/selected-ion flow tube (ICP-SIFT) [9]. They found a 748 kJ mol^{-1} value and, as above mentioned, our is lower than theirs by 63 kJ mol^{-1} because of the overestimation of $\Delta H_f(ZrO^+)$ with the Lanl2DZ++* basis set. This one also affects OA(^+ZrO), the oxygen atom affinity of ZrO^+, leading to a value higher than the experimental one deduced from Sievers and Lias data [15,20]. As regards the strontium species, the computed OA(Sr^+) is in good agreement with the value reported by Schröder et al. [28] ($\delta OA = 16$ kJ mol^{-1}) and our DFT calculations give a first determination of the O-atom affinity of strontium monoxide, OA(^+SrO) = 83 kJ mol^{-1}. The comparison of the computed OA values confirms that Zr^+ and its oxide have a greater affinity for oxygen than Sr^+ and SrO^+. The smaller bond lengths obtained for zirconium oxides ($d(^+Zr–O) = 1.68$ Å, $d(O^+Zr–O) = 1.78$ Å) than for strontium

oxides ($d(^+Sr–O) = 2.17$ Å, $d(O^+Sr–O) = 2.35$ Å), prove stronger binding interactions. They are consistent with the results on OA and with the behavior of ions in the collision-reaction cell. High oxygen affinity values obtained for zirconium species explain why ZrO^+ and ZrO_2^+ are observed as of oxygen introduction in the cell and still for higher flow rate contrary to SrO^+ and SrO_2^+. The Zr–O bonds formed are strong enough to resist the collisions with the most energetic oxygen molecules, corresponding to highest flow rate, which is not the case for Sr–O bonds.

In addition the endothermic/exothermic characters of the reactions are qualitatively confirmed by our computed enthalpies. Reactions (3) and (4) of oxygen with Zr^+ are definitely exothermic ($\Delta H_r < 0$), while significantly positive ΔH_r value are obtained for Sr^+. The comparison of $[P_{O_2}]_{1/2}$ values obtained for the O_2-condensation reaction (4) (respectively, 3×10^{-110} and 3×10^{11} bar for reactions relative to Zr and Sr) with that found experimentally in the cell gives also information on the different behavior of zirconium and strontium. The pressure orders of magnitudes are obviously out of proportion, but they illustrate in a simple way the completely different behaviors of Zr^+ and Sr^+ ions. Indeed for usual O_2 flow rate (<1 mL min^{-1}) the pressure in the cell is around 10^{-5} bar, largely below the 3×10^{11} bar necessary to the reaction of Sr^+. According to these results, the reaction concerning Zr^+ will proceed immediately while it will not for Sr^+, evidencing that zirconium is stabilized under the ZrO_2^+ form (Fig. 3) and confirming this way the conclusions of the thermodynamics. To our best knowledge no value was published for the formation enthalpy of SrO_2^+, $\Delta H_f(SrO_2^+)$. Our DFT calculations provide a way for accessing to a first value of this thermodynamic quantity. Since a reasonable ΔH_r value of reaction (4) relative to Zr was obtained by using the DFT method with the Lanl2DZ++* basis set as compared to experimental determination (respectively, -649 and -639 kJ mol^{-1}, Table 5), we used our energy calculated for the SrO_2^+ system to evaluate $\Delta H_f(SrO_2^+)$ according to equation

$$\Delta H_{rDFT} = \Delta H_f(SrO_2^+) - \Delta H_f(Sr^+)_{exp} - \Delta H_f(O_2)_{exp} \quad (c)$$

$\Delta H_{r\,DFT}$ is the reaction enthalpy obtained from DFT calculations with the Lanl2DZ++* basis set, $\Delta H_f(Sr^+)_{exp}$ and $\Delta H_f(O_2)_{exp}$ experimental data [15]. The value 846 kJ mol^{-1} was thus found as an estimation of the SrO_2^+ formation enthalpy at 298 K.

3.4. Experimental insight

Proportions of each species were measured for different molecular oxygen flow rates to experimentally confirm the above theoretical predictions on zirconium and strontium behavior.

The graph in Fig. 4 evidences differences in reactivity of the two species towards oxygen as anticipated by the calculations. Zirconium oxides were indeed observed in great proportions when introducing oxygen. Even at a very low flow rate (0.1 mL min^{-1}), where the partial pressure of O_2 was still low, we measured the apparition of ZrO^+, which already represented 70% of total zirconium, while the proportion of Zr^+ ions was less than 10%. The higher oxides formed as the gas flow rate was increased. This can be interpreted as a result of the

Table 5
Comparison of experimental and calculated reaction enthalpies, ΔH_r, at $T = 298$ K, $P = 1$ atm (enthalpies are in kJ mol^{-1})

	ΔH_r-Zr		ΔH_r-Sr	
	Experimental[a]	Lanl2DZ++*	Experimental[a]	Lanl2DZ++*
$M^+ + O_2 \rightarrow MO^+ + O$ (reaction (3))	−249	−186	+199	+215
$M^+ + O_2 \rightarrow MO_2^+$ (reaction (4))	−639	−649	na[b]	+133

[a] Derived from heats of formation tabulated in Refs. [15,20].

[b] Not available because no value is published for $\Delta H_f(SrO_2^+)$.
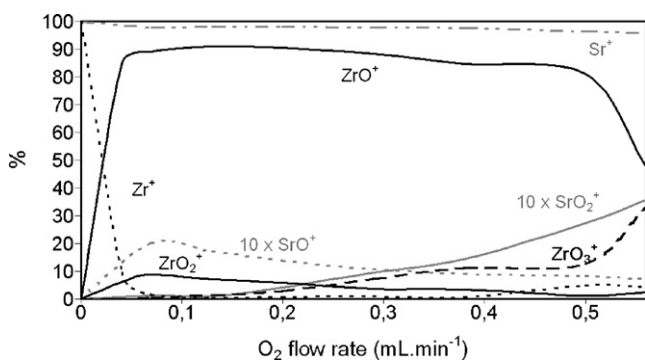
Fig. 4. Zirconium and strontium oxides repartition according to the oxygen flow rate.

kinetic effect of the corresponding increase of P_{O_2}. Conversely, even for the highest considered oxygen flow rate (0.6 mL min^{-1}) the cumulative percentage of strontium oxides was still less that 4%. Indeed strontium monoatomic ion is always largely prevailing, proof of the strontium non-reactivity towards oxygen. Strontium oxides formed at highest oxygen flow rates can be explained by a supplementary energy contribution, leading to an increase of the collision energy, which certainly compensates for the endothermic barrier of the reaction. The axial kinetic energy of the O_2 molecules or the energy coming from possible excited states of Sr$^+$ ions can bring this additional contribution. In addition, even if no experimental data was available, it was correct to anticipate an endothermic character ($\Delta H_r > 0$) for the O_2-condensation reaction of Sr$^+$ according to our theoretical results. Indeed almost no SrO$_2^+$ was formed in the cell.

4. Conclusion

In this study, utility of DFT calculations was shown for modeling ion–gas reactions in the collision-reaction cell of an ICP-MS through the isobaric interference ^{90}Zr–^{90}Sr solved by using O_2 as the reaction gas. The two interfered ions, Zr$^+$ and Sr$^+$, have a completely different behavior with oxygen, which is taken advantage for solving the interference. Ground state spin multiplicities S and equilibrium geometries of each species involved in the oxidation reactions were determined. The completely different stabilities of zirconium and strontium oxides were explained by the nature of the chemical bonding in these species. Certain thermodynamic values already available in literature, like O-atom affinities, OA, were reproduced with sufficient accuracy for giving an explanation of polyatomic ions' behavior in the cell. The comparison of computed reaction enthalpies correctly predicted that zirconium oxides formed in

the cell while strontium oxides did not, allowing strontium measurement at mass 90. But employed methods do not seem to be completely adapted to the ZrO$^+$ calculation, even if using our augmented basis set Lanl2DZ++* improved some theoretical values in comparison of the first results reported elsewhere [18]. Maybe a wider basis set should be used to take into account electron exchange of O towards Zr empty d orbitals. However, above results show that DFT method allows to qualitatively model reactions in the field of the mass spectrometry as initially envisaged.

References

[1] V.F. Taylor, R.D. Evans, R.J. Cornett, Anal. Bioanal. Chem. 387 (2007) 343.
[2] H. Isnard, M. Aubert, P. Blanchet, R. Brennetot, F. Chartier, V. Geertsen, F. Manuguerra, Spectrochim. Acta Part B 61 (2006) 150.
[3] A.P. Vonderheide, M.V. Zoriy, A.V. Izmer, C. Pickhardt, J.A. Caruso, P. Ostapczuk, R. Hille, J.S. Becker, J. Anal. At. Spectrom. 19 (2004) 675.
[4] F. Vanhaecke, Anal. Bioanal. Chem. 372 (2002) 20.
[5] S.D. Tanner, J. Anal. At. Spectrom. 10 (1995) 905.
[6] S.D. Tanner, V.I. Baranov, D.R. Bandura, Spectrochim. Acta Part B 57 (2002) 1361.
[7] D.R. Bandura, V.I. Baranov, S.D. Tanner, Fresenius J. Anal. Chem. 370 (2001) 454.
[8] G.C. Eiden, J. Barinaga, D.W. Koppenaal, Rapid Commun. Mass Spectrom. 11 (1997) 37.
[9] G.K. Koyanagi, D. Caraiman, V. Blagojevic, D.K. Bohme, J. Phys. Chem. A 106 (2002) 4581.
[10] B. Hattendorf, D. Günther, Spectrochim. Acta Part B 58 (2003) 1.
[11] M.J. Frisch, G.W. Trucks, H.B. Schlegel, G.E. Scuseria, M.A. Robb, J.R. Cheeseman, J.A. Montgomery Jr., T. Vreven, K.N. Kudin, J.C. Burant, J.M. Millam, S.S. Iyengar, J. Tomasi, V. Barone, B. Mennucci, M. Cossi, G. Scalmani, N. Rega, G.A. Petersson, H. Nakatsuji, M. Hada, M. Ehara, K. Toyota, R. Fukuda, J. Hasegawa, M. Ishida, T. Nakajima, Y. Honda, O. Kitao, H. Nakai, M. Klene, X. Li, J.E. Knox, H.P. Hratchian, J.B. Cross, C. Adamo, J. Jaramillo, R. Gomperts, R.E. Stratmann, O. Yazyev, A.J. Austin, R. Cammi, C. Pomelli, J.W. Ochterski, P.Y. Ayala, K. Morokuma, G.A. Voth, P. Salvador, J.J. Dannenberg, V.G. Zakrzewski, S. Dapprich, A.D. Daniels, M.C. Strain, O. Farkas, D.K. Malick, A.D. Rabuck, K. Raghavachari, J.B. Foresman, J.V. Ortiz, Q. Cui, A.G. Baboul, S. Clifford, J. Cioslowski, B.B. Stefanov, G. Liu, A. Liashenko, P. Piskorz, I. Komaromi, R.L. Martin, D.J. Fox, T. Keith, M.A. Al-Laham, C.Y. Peng, A. Nanayakkara, M. Challacombe, P.M.W. Gill, B. Johnson, W. Chen, M.W. Wong, C. Gonzalez, J.A. Pople, GAUSSIAN 03, Revision B. 05, Gaussian Inc., Pittsburgh, PA, 2003.
[12] A.D. Becke, J. Chem. Phys. 98 (1993) 5648.
[13] D. Andrae, M. Häussermann, M. Dolg, H. Soll, H. Preuss, Theor. Chim. Acta 77 (1990) 123.
[14] P.J. Hay, W.R. Wadt, J. Chem. Phys. 82 (1985) 270.
[15] S.G. Lias, J.E. Bartmess, J. Phys. Chem. Ref. Data 17 (Suppl. 1) (1988).
[16] P. Flükiger, H.P. Lüthi, S. Portmann, J. Weber, MOLEKEL 4. 0, Swiss Center for Scientific Computing, Manno, Switzerland, 2000.
[17] S. Portmann, H.P. Lüthi, Chimia 54 (2000) 766.
[18] F. Rondinelli, N. Russo, M. Toscano, Theor. Chem. Acc. 115 (2006) 434.

[19] V.V. Lavrov, V. Blagojevic, G.K. Koyanagi, G. Orlova, D.K. Bohme, J. Phys. Chem. A 108 (2004) 5610.

[20] M.R. Sievers, Y.-M. Chen, P.B. Armentrout, J. Chem. Phys. 105 (1996) 6322.

[21] M.R. Sievers, P.B. Armentrout, Int. J. Mass Spectrom. 185/186/187 (1999) 117.

[22] R.J. Van Zee, S. Li, W. Weltner Jr., Chem. Phys. Lett. 217 (1994) 381.

[23] P.E.M. Siegbahn, J. Phys. Chem. 97 (1993) 9096.

[24] M.M. Kappes, R.H. Staley, J. Phys. Chem. 85 (1981) 942.

[25] N. Godbout, D.R. Salahub, J. Andzelm, E. Wimmer, Can. J. Chem. 70 (1992) 560.

[26] S. Huzinaga, M. Klobukowski, Chem. Phys. Lett. 212 (1993) 260.

[27] L.A. LaJohn, P.A. Christiansen, R.B. Ross, T. Atashroo, W.C. Ermler, J. Chem. Phys. 87 (1987) 2812.

[28] D. Schröder, H. Scwharz, S. Shaik, Structure and Bonding, vol. 97, Springer-Verlag, Berlin, 2000.